Journal of Thermal Analysis, Vol. 45 (1995)1381-1392

THERMOANALYTICAL INVESTIGATION OF THE DECOMPOSITION COURSE OF COPPER OXYSALTS

II. Copper(II) nitrate trihydrate

S. A. A. Mansour

Chemistry Department, Faculty of Science, Minia University, El-Minia, Egypt

(Received February 14, 1994; in revised form December 20, 1994)

Abstract

The thermal decomposition of copper nitrate trihydrate (CuNTH); $Cu(NO_3)_2 \cdot 3H_2O$ was studied up to 600°C by thermogravimetry (TG) and differential thermal analysis (DTA) in a dynamic atmosphere of air. The thermal events occurring throughout the decomposition course were characterized on the basis of spectral analyses using infrared spectroscopy (IR), X-ray diffractometry (XRD) and scanning electron microscopy (SEM). Non-isothermal kinetic parameters were determined. The results showed that the decomposition course involves two main processes, firstly the formation of hydroxy copper nitrate and secondly, the decomposition of this compound to yield CuO. Pathways were suggested that may be involved in the decomposition course.

Keywords: copper oxysalts

Introduction

Supported copper and copper oxide are powerful catalysts in methanol synthesis [1–3], in partial stereoselective hydrogenation of alkanes [4] and in reduction of nitric oxide [5]. The common preparation method of such industrially important catalysts involves the thermal decomposition at suitable temperature of copper nitrate precursor, previously supported on an inert carrier [6]. In such preparation methods, knowledge of the degradation processes and the thermal interactions of the precursor are of great value.

Studies of the thermal decomposition of metal nitrates have been reported [7] to be complicated because of the possibility of interaction of the evolved nitrogen oxides and/or the occurrence of phase transition in the early stages of decomposition. Hence, the adoption of a dynamic technique under a flow of gas, would help to keep these complications to the minimum.

The present study was carried out to investigate the thermal decomposition course of copper nitrate trihydrate using thermogravimetric and differential thermal analysis techniques under a dynamic atmosphere of air. Non-isothermal

0368–4466/95/ $ 5.00

John Wiley & Sons, Limited
Chichester

kinetic parameters have been calculated. The solid decomposition products obtained at intermediate temperatures were analysed by infrared spectroscopy, X-ray diffractometry and scanning electron microscopy.

Experimental

Material

The copper nitrate trihydrate (CuNTH); $Cu(NO_3)_2 \cdot 3H_2O$ used was an AR-grade highly pure (BDH) product. Portions of the material were calcined for 2 h in a stationary atmosphere of air at temperatures chosen on the basis of thermal analysis results (see below). The solid products of calcination were kept dry for further analysis.

Apparatus and methods

Thermogravimetric (TG) and differential thermal analysis (DTA) were performed with an automatically recording Shimadzu Thermal Analyzer Unit (Model 30H, Japan). TG and DTA curves were recorded at four heating rates (θ=2, 5, 10 and 20 deg·min^{-1}) in a dynamic (30 ml·min^{-1}) atmosphere of air. The sample size was ca 10 mg for TG, while highly sintered α-Al_2O_3 was used as a reference material for DTA. Calculations of the kinetic parameters were carried out on the basis of Ozawa's method [8] as described earlier [9].

Infrared spectroscopic analysis (IRA) of CuNTH and its solid calcination products was carried out over the range 4000–300 cm^{-1}, at a resolution of 5.3 cm^{-1}, by means of a Model 580B Perkin-Elmer spectrophotometer (UK). The spectra were taken from thin (< 20 mgcm^{-2}) lightly loaded (< 1%) KBr supported discs of the test samples.

X-ray diffractometry (XRD) of CuNTH and its calcination products was performed using a Model JSX-60 PA Jeol diffractometer (Japan), equipped with a source of Ni-filtered CuK$_\alpha$ radiation. The obtained diffraction patterns [I/I_o *vs.* d–spacing (Å)], were matched with ASTM standards for identification.

Morphological changes occurring during the progress of CuNTH decomposition were investigated using a Jeol 35 CF scanning electron microscope (SEM). Samples of CuNTH and its calcination products were mounted for viewing and rendered conducting by coating lightly with gold. The photographs presented here illustrate typical and reproducible structures that are considered to be significant.

Results and discussion

The TG and DTA curves recorded for CuNTH at 10 deg·min^{-1} in a dynamic (30 ml·min^{-1}) atmosphere of air are shown in Fig. 1. The Figure indicates that

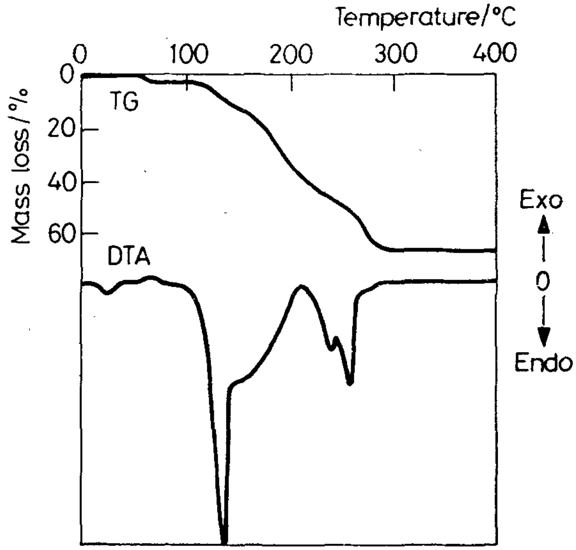

Fig. 1 TG and DTA curves of CuNTH recorded at a heating rate of 10°C·min^{-1} in a dynamic atmosphere of air (30 ml·min^{-1})

CuNTH decomposes via three endothermic mass loss events, namely II, III and IV, with maxima at 135, ~160 and 255°C. An earlier endothermic mass-invariant event, I is clear from the DTA curve, with a maximum at 50°C. The T_{max} shifts experienced for the mass-loss events as a function of the heating rate (θ=2–20 deg·min^{-1}) are indicated in Fig. 2.

Figures 3 and 4 show the IR spectra and X-ray powder diffractograms obtained for CuNTH and its calcination products at 170–600°C.

The non-isothermal kinetic parameters (k, A, ΔE) determined for the thermal events encountered throughout the decomposition course of CuNTH are compiled in Table 1.

Logθ *vs.* $1/T_{max}$ plots constructed for the thermal events are shown in Fig. 5.

Characterization of the thermal events observed

Thermal event I

Thermal event I (Fig. 1) is an endothermic mass invariant process, with a maximum at 50°C. The material showed no response to DSC measurement in this temperature range, hence, event I could not be attributed to melting. Therefore, it seemed reasonable to attribute event I to a sort of phase transition. The possibility of the occurrence of such transition in the early stages of the thermal decomposition of metal nitrates has been reported [10].

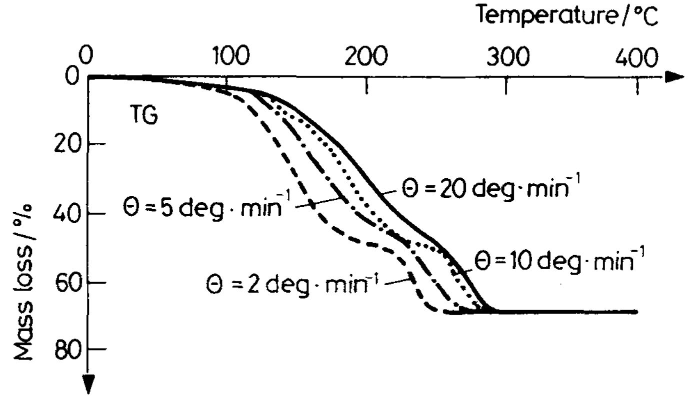

Fig. 2 TG curves of CuNTH as a function of heating rate in a dynamic (30 ml·min^{-1}) atmosphere of air

Thermal events II and III

Thermal events II and III are shown by the TG and DTA curves of CuNTH (Fig. 1) to be overlapping endothermic mass-loss processes, with maxima at 135 and ca 160°. The IR spectrum of the calcination product obtained at 170°C (Fig. 3) displays almost all the absorption bands of the parent CuNTH except for the appearance of new resolved absorption bands at 500 and 410 cm^{-1} which may be due to Cu–O vibrations [11, 12]. The X-ray diffractogram of the calcination product at 170°C (Fig. 4) shows a pattern different from that of the parent CuNTH in displaying the characteristic lines of copper nitrate hydroxide (ASTM Card no. 15–14) as a major component. The diffractogram exhibits also, in rather low intensities, the characteristic lines of the parent CuNTH (ASTM Card no. 21–296) as well as those of CuO (ASTM Card no. 5–661).

The IR spectrum of the calcination product obtained at 200°C (Fig. 3) exhibits some differences from that of the parent salt, however, it still displays the absorption bands of the nitrate. The spectrum exhibits two new bands at 1420 and 1340 cm^{-1}. These two bands are considered to be due to the splitting of the ν_3 (at 1380 cm^{-1}) absorption which is diagnostic of the highly symmetric ionic nitrates [13]. Hence the absorption bands at 1420 and 1340 cm^{-1} could be assigned as the ν_4 and ν_1 components of ν_3. It has been suggested [13] that the difference between ν_4 and ν_1, (Δ) may be taken as a measure of the dissymmetry arising in the nitrate group as a result of an increase in the degree of covalency. The spectrum also indicates the splitting of the absorption band at 820 cm^{-1}, which could be attributed to the same reason of dissymmetry.

The calcination product obtained at 200°C shows an XRD pattern (Fig. 4) quite similar to that obtained at 170°C. The pattern reveals a marked increase in

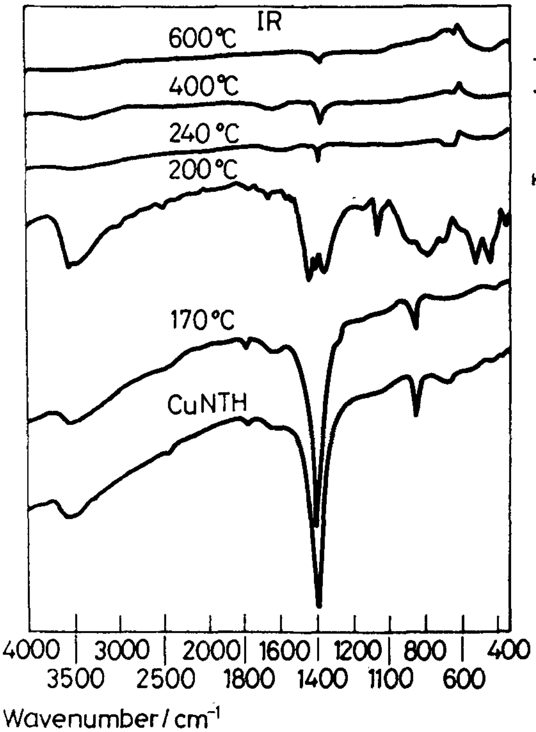

Fig. 3 IR spectra of CuNTH and its calcination products at the temperatures indicated for 2 h

the characteristic lines of CuO. This should indicate the increase in the CuO content in this calcination product. From these results together with the fact that CuNTH melts at about 115°C [14], thermal event II could be attributed to the melting process. Such melting, in addition to the water content of the salt would presumably facilitate the occurrence of hydrolysis followed by the formation of hydroxy copper nitrate intermediate, which partly dissociates giving rise to CuO at the onset of the final decomposition process (event IV). Accordingly, processes involved in these two events [II and III] can be visualized as follows:

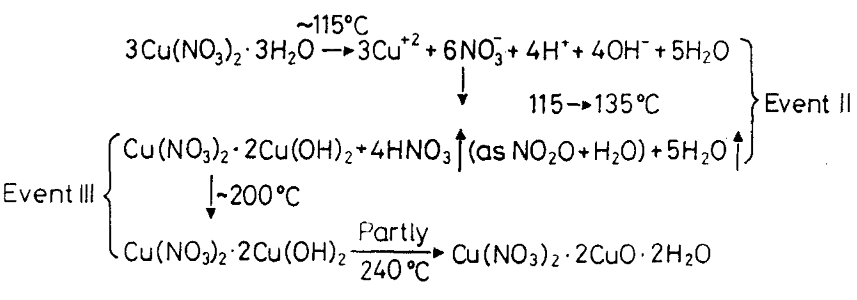

$$\left.\begin{array}{l}3Cu(NO_3)_2\cdot 3H_2O \xrightarrow{\sim 115^\circ C} 3Cu^{+2} + 6NO_3^- + 4H^+ + 4OH^- + 5H_2O \\ \qquad\qquad\qquad\qquad \downarrow \; 115 \rightarrow 135^\circ C \\ Cu(NO_3)_2\cdot 2Cu(OH)_2 + 4HNO_3\uparrow (\text{as } NO_2O + H_2O) + 5H_2O\uparrow\end{array}\right\} \text{Event II}$$

$$\text{Event III}\left\{\begin{array}{l}Cu(NO_3)_2\cdot 2Cu(OH)_2 + 4HNO_3\uparrow (\text{as } NO_2O + H_2O) + 5H_2O\uparrow \\ \downarrow \sim 200^\circ C \\ Cu(NO_3)_2\cdot 2Cu(OH)_2 \xrightarrow[240^\circ C]{\text{Partly}} Cu(NO_3)_2\cdot 2CuO\cdot 2H_2O\end{array}\right.$$

In support of these results, the IR spectrum of the calcination product obtained at 240°C (Fig. 3) reveals a marked decrease in the intensity of the absorption band of the nitrate ion at 1380 cm^{-1}. On the other hand, the total mass loss accompanying events II and III (i.e. up to 240°) amounts to 48% which is equal to the value calculated for the transformation $3Cu(NO_3)_2 \cdot 3H_2O \rightarrow Cu(NO_3)_2 \cdot Cu(OH)_2$. The activation energies (ΔE) of these two events were found to be 118 and 102 $kJ \cdot mol^{-1}$ for events II and III, respectively (Table 1).

Table 1 Non-isothermal kinetic parameters of the thermal events (I–IV) encountered throughout the decomposition course of CuNTH, calculated from TG and DTA data

Thermal event	ΔE/kJ·mol^{-1}	k/min^{-1}	log A
I	60	–	–
II	118	2.9×10^{-2}	13.7
III	102	14.0×10^{-2}	10.6
IV	155	54.4×10^{-2}	14.6

Thermal event IV

Figure 1 indicates that thermal event IV is endothermic with a maximum at 255°C, involving a mass loss of 19.5% which brings the total mass loss to 67.5%, very close to that expected (67%) for the decomposition of $Cu(NO_3)_2 \cdot 3H_2O$ to CuO. Thus, event IV involves primarily the decomposition of the hydroxy nitrate intermediate to CuO. The IR spectrum of the calcination product obtained at 400°C (Fig. 3) exhibits bands due to CuO (at 610, 500 and 410 cm^{-1}) [11, 12]. The spectrum (Fig. 3) shows a weak band due to nitrate at 1380 cm^{-1}. This particular band is also shown at 600°C (Fig. 3), but is much weaker intensity. The persistence of this band indicates an incomplete removal of the nitrate. Such nitrate could be either a strongly adsorbed surface species and/or a nitrate component that perhaps had become trapped within the porous structure of the developing CuO.

The X-ray diffractograms of the calcination products formed at 400 and 600°C (Fig. 4) exhibit the pattern that is documented for CuO (ASTM Card no. 5–661). The crystallinity is shown to improve with rising temperature. The activation energy value (ΔE) of this event amounts to 155 $kJ \cdot mol^{-1}$ (Table 1), which is expected for such decomposition reactions. It is to be noted that the DTA curve (Fig. 1) shows a multi-step peak for event IV which may indicate the complexity of the solid material involved in this process [$Cu(NO_3)_2 \cdot 2Cu(OH)_2$]. Hence, the following reaction may be involved in thermal event IV:

$$Cu(NO_3)_2 \cdot 2Cu(OH)_2 \rightarrow 3CuO + 2NO_2 + 2H_2O + 1/2O_2$$

The release of NO_2 in this last decomposition step could reasonably account for the presence of an infrared absorption band of nitrate, possibly as adsorbed species.

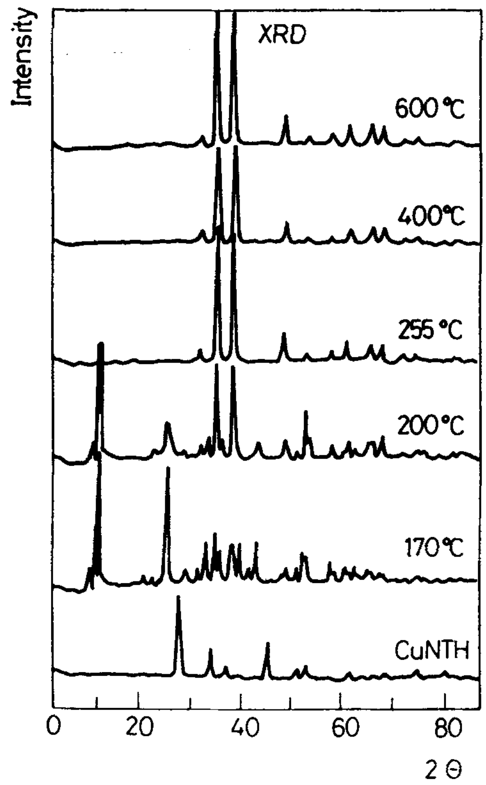

Fig. 4 X-ray powder diffractograms of CuNTH and its calcination products at the temperatures indicated for 2 h

The above results permit the following conclusions:

1) The thermal decomposition of copper nitrate trihydrate may include the following pathways:

$$(Cu(NO_3)_2\cdot 3H_2O)(s) \xrightarrow{I} (Cu(NO_3)_2\cdot 3H_2O)(s')$$

$$\begin{tikzcd}
3(Cu(NO_3)_2\cdot 3H_2O)(s') \arrow[r, "II"] & 3Cu^{+2}+6NO_3^- +4H^+ +4OH^- +5H_2O \arrow[d, "III"] \\
3CuO+2NO_2\uparrow+2H_2O\uparrow+1/2O_2\uparrow & Cu(NO_3)_2\cdot 2Cu(OH)_2+O_2\uparrow+7H_2O\uparrow+4NO_2\uparrow \arrow[l, "IV"']
\end{tikzcd}$$

where *s* and *s'* indicate solid materials and the roman numerals denote the accompanying thermal events.

2) The final decomposition product (CuO) was found to be contaminated by a minute amount of nitrate which persists on further heating (up to 600°C).

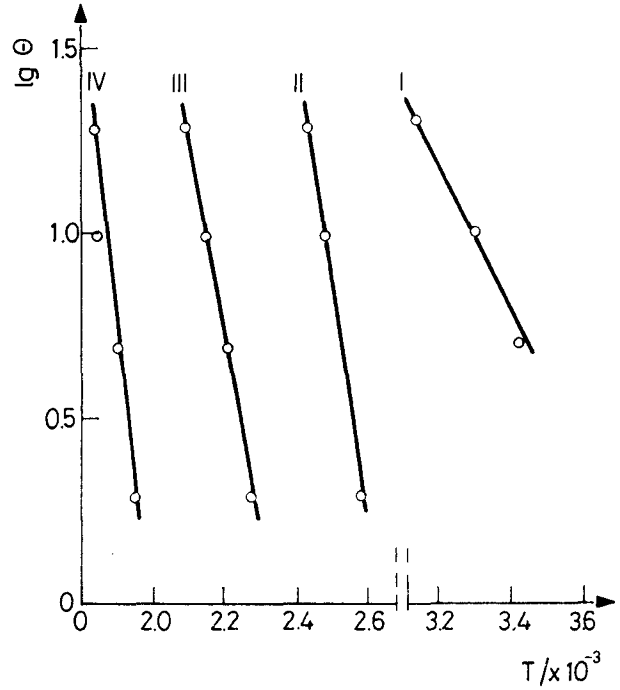

Fig. 5 Logθ *vs.* $1/T_{max}$ plots derived for thermal events encountered throughout the decomposition of CuNTH

Electron microscopic examinations

Attempts were made to correlate the morphological changes accompanying the decomposition of CuNTH with the corresponding physicochemical data. Unfortunately, the parent salt and the calcination products at 170 and 200°C suffered a severe change by the electron beam in spite of the coating. However, the parent salt was composed mainly of a wide size-range of well-formed crystals with flat smooth surfaces. The crystals were large enough to be seen with the naked eye and deliquesced when left in air at room temperature.

The calcination product obtained at 240°C appeared as agglomerates of very fine crystals (Fig. 6a). This product, as indicated by the results of thermal analysis, has been formed from molten phase. However, the intermediate formed has a reproducible structure. A typical crystal is shown in Fig. 6b. This calcination product appeared as irregular aggregates of crystallites (Fig. 6c).

Heating up to 400°C resulted in the appearance of cleavages as shown in Fig. 7a, as well as formation of new crystallites of CuO (Fig. 7b) which were

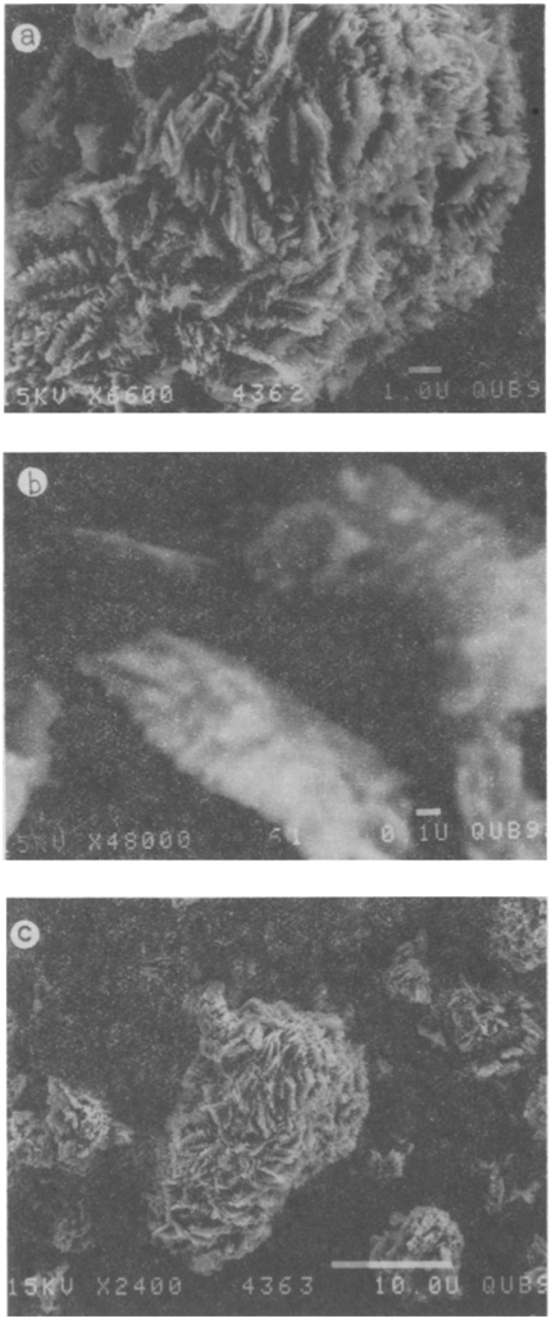

Fig. 6 Scanning electron micrographs of the calcination product of CuNTH at 240°C showing assemblage of the produced crystals (a), created crystals (b) and agglomeration of grains (c)

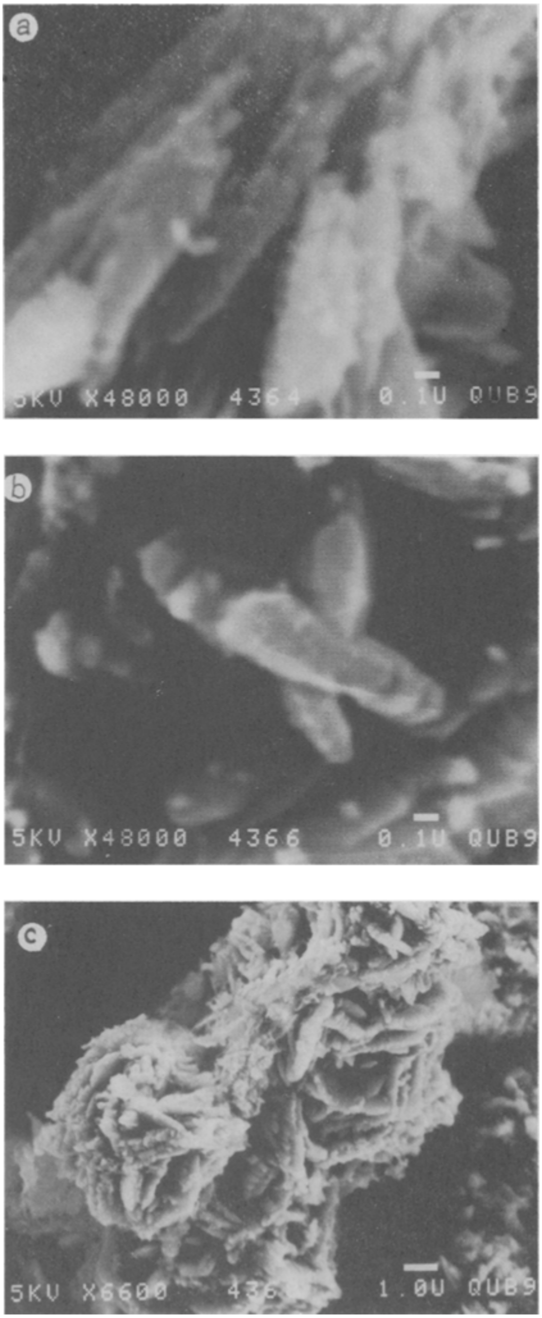

Fig. 7 Scanning electron micrographs of CuNTH calcined at 400°C revealing crystals cleavages (a), creation of new crystals (b), and assemblage of the produced crystals (c)

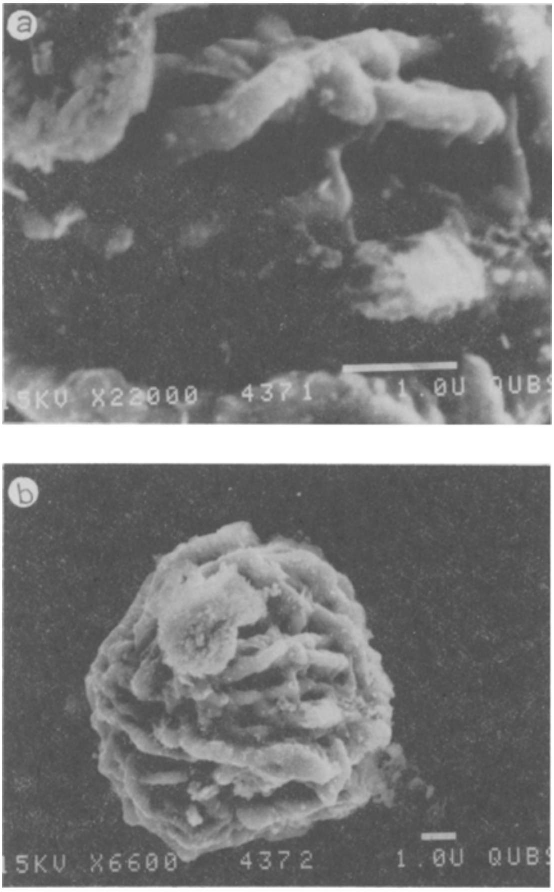

Fig. 8 Scanning electron micrographs of the final decomposition product revealing the created crystals (a) and typical product grains (b)

pseudomorphic with the previous calcination product. These new crystals preserved the original aggregation as indicated by Fig. 7c.

Increasing the calcination temperature up to 600°C gave rise to a greater degree of crystallinity. Figure 8a shows a sign of crystal growth. The final decomposition product appeared as aggregates of coherent crystals (Fig. 8b). The XRD pattern was in good agreement with these observations where the crystallinity improved with increasing calcination temperature.

* * *

It is a pleasure to thank the Queen's University of Belfast, particularly the staff of the Electron Microscope Unit for assistance in obtaining the electron micrographs. Thanks also are due to the Egyptian Government for the granted fellowship.

References

1 M. Lo Jacono and M. Schiavello, in Preparation of Catalysts, (B. Delman, P. A. Jacobs and G. Poneelet, Eds.), Elsevier, Amsterdam, 1976, pp. 474–487.
2 E. D. Pierron, J. A. Rashkin and J. F. Roth, J. Catal., 9 (1967) 38.
3 R. M. Friedman, J. J. Freeman and F. W. Lytle, J. Catal., 55 (1978) 10.
4 A. Wolberg and J. F. Roth, J. Catal., 15 (1969) 250.
5 Pope, C. Angeletti, S. De Rossi and M. La Jacono, J. Catal., 91 (1985) 69.
6 D. I. Trimm. Design of Industrial Catalysts. Chemical Engineering monographs. Elsevier. New York, 1980.
7 W. E. Brown, D. Dolimore and A. K. Galwey, in C. H. Bamford and C. F. H. Tipper (Eds.), Chemical Kinetics, Vol. 22. Reactions in the Solid State. Elsevier, Amsterdam 1980, p. 182.
8 T. Ozawa, J. Thermal Anal., 2 (1970) 301.
9 S. A. A. Mansour, Thermochim. Acta, 228 (1993) 156.
10 A. C. McLaren, Rev. Pure Appl. Chem., 12 (1962) 54.
11 N. T. Mcdevitt and E. L. Baun, Spectrochim. Acta, 20 (1964) 799.
12 F. F. Bently, L. D. Smithson and A. L. Rozek, Infrared Spectra and Characteristic Frequencies ~700–300 cm^{-1}, Wiley, USA 1968, p. 1517.
13 K. C. Taylor, in J. R. Anderson and M. Baudart (Editors), Catalysis-Science and Technology, Vol. 5, Springer-Verlag, Berlin, 1984, pp. 120–165.
14 R. C. Weast (Editor), Handbook of Chemistry and Physics, CRC Press, Boca Raton, Florida, 62nd edn., 1981.

Zusammenfassung — Mittels Thermogravimetrie (TG) und Differentialthermoanalyse (DTA) in dynamischer Luftatmosphäre wurde der thermische Zersetzungsweg von Kupfernitrattrihydrat (CuNTH); $Cu(NO_3)_2 \cdot 3H_2O$ bis zu einer Temperatur von 600°C untersucht. Die während des Zersetzungsvorganges ablaufenden thermischen Ereignisse wurden auf der Grundlage von Spektralanalyse mittels Infrarotspektroskopie (IR), Röntgendiffraktion (XRD) und Scanning-Elektronenmikroskopie (SEM) charakterisiert. Nichtisotherme kinetische Parameter wurden ermittelt. Die Ergebnisse zeigten, daß die Zersetzung zwei Hauptprozesse umfaßt, als erstes die Bildung von Hydroxy-Kupfernitrat und zweitens, die Zersetzung dieser Verbindung zu CuO. Es wurden Wege vorgeschlagen, die bei dieser Zersetzung involviert sein können.